IEEE Access
Multidisciplinary | Rapid Review | Open Access Journal

Received December 7, 2019, accepted January 11, 2020, date of publication January 20, 2020, date of current version February 28, 2020.

Digital Object Identifier 10.1109/ACCESS.2020.2968089

Geophone-Based Energy Harvesting Approach for Railway Wagon Monitoring Sensor With High Reliability and Simple Structure

WEI HE[1], WEIZHONG SHI[2], JIANWEI LE[2], HUI LI[3], AND RUNZE MA[1]
[1]Shanghai Institute of Microsystem and Information Technology, Chinese Academy of Science, Shanghai 200050, China
[2]China Railway Information Technology Company, Ltd., Beijing 100038, China
[3]Fujian Fuzhou Railway Local Railway Development Company, Ltd., Fuzhou 350013, China

Corresponding author: Runze Ma (marunze@mail.sim.ac.cn)

This work was supported in part by the National Key Research and Development Program of China under Grant 2018YFC1505204-2, and in part by the CAS Key Deployment Project under Grant KFZD-SW-431.

ABSTRACT Freight train positioning and axle safety monitoring are the key to railway traffic supervision, which can be achieved by sensors based on Internet of Things (IoT) technology, and the energy harvesting technology is the best solution to those sensors due to neither electrical power nor communication system is available on railway wagons. This paper proposes a self-powered railway wagon monitoring sensor (SpRWMS) solution based on the geophone, which has the characteristics of mature technology and simple structure, and can convert mechanical vibration of wagons into electrical energy. Since the vibration is so weak that the voltage induced by the geophone is very weak, hence, this paper proposes an electromagnetic generator (EMG) constructed by geophone matrix and an energy management interface (EMI) to convert the induced potential into the voltage that can drive the circuit system of sensors. In this paper, the implementation and performance of EMI will be focused on, and the energy harvesting system analysis prior to developing prototypes and conducting field trail. The design principles and prototypes of EMG and EMI are proposed based on the parameters of vibration profiles collected by a data logger, and the performance of the SpRWMS prototype is evaluated on a trial run freight train. Experimental results show that the proposed EMI can extract the energy generated by EMG more effectively and increase the voltage across the storage capacitor from 2V to 3.3V, that is, our proposed EMI and EMG can convert the railway wagon vibrational energy into the electrical energy form required by the circuitry of sensors.

INDEX TERMS Energy harvesting, Internet of Things, vibration.

I. INTRODUCTION

At present, more and more IoT-based sensors with different functions are attached on the wagons of freight trains to achieve position, axle temperature, axle crack monitoring, etc. However, in all the carriages of traditional freight trains, there is neither electricity nor communication systems [1]. Hence, batteries are used to supply electrical energy to these sensors. In order to avoid frequent replacement of batteries assembled in these sensors, energy harvesting techniques based on solar cells and micro winds were proposed in [2] and [3], respectively. However, neither of these techniques is suitable for the harsh operating conditions of freight trains due to the influence of rain, fog, dust, etc.

The associate editor coordinating the review of this manuscript and approving it for publication was Giacomo Verticale.

In those monitoring scenarios such as wagon location and security, mechanical vibration energy generated by the interaction of train wheels and rails is the most promising source in this case to power railway wagon monitoring sensors (RWMSs) based on the Internet of Things [4]– [5]. Generally, there are two main mechanisms to convert the mechanical vibration energy into the electrical energy: piezoelectric [6]–[8] and electromagnetic principle [6], [9]. Nevertheless, it is not easy to extract energy from such a source due to the vibration caused by the freight trains changes with time in terms of frequency and amplitude [10]. Therefore, many researches focus on improving the efficiency of power generation by improving material properties and manufacturing processes.

A piezoelectric generator (PEG) which can generate $40.245\mu W/cm^3$ on a passenger train was designed in [11].

According to the same principle, [12] has experimented their proposed piezoelectric converter with different cantilever beam thicknesses and different piezoelectric material dimensions on an operating commercial high-speed Korean train with a speed greater than 300km/h, and found that the converter can generate 19.64mW when 8 permanent magnets were added as tip mass on the cantilever. Additionally, literature [13] has utilized piezoelectric materials to design a power generation device and provided power supply for the axle temperature sensor to provide safety monitoring for the carriages of freight trains. The results of those studies showed that the energy harvesting technology based on the piezoelectric principle can obtain electric energy in the range of mJ from the vibration of freight train cars, and can provide sufficient energy supply for the RWMSs with the appropriate power management module (PMM). These studies have important guiding significance for the future research of energy harvesting technology based on piezoelectric principle.

However, it can be seen from the literature [11] to [13] that the efficiency of energy harvesting devices is realized by changing the characteristics of piezoelectric material, as well as a large and complex mechanical support structure, which is very difficult for the electronics engineers. Moreover, due to the lack of uniform process standards, the reliability and performance of those energy harvesting devices will be severely affected [14]. Therefore, this type of energy harvesting devices is not suitable for the RWMSs with reliability requirements.

Vibration energy harvesting technology based on the electromagnetic principle has also attracted researchers' attention over the past decade due to its high energy density. An electromagnetic generator (EMG) mounted on the rail was developed to obtain the vibrational energy excited by the passing trains and to power sensors was proposed in [15]. Moreover, an electromagnetic generator was designed and implemented in [1], which can generate electric energy with maximum voltage of 1.7V peak-to-peak and maximum power of 10mW output. In addition, theoretical analysis of energy harvesting techniques based on electromagnetic principles was carried out in [10] and [6].

Generally, PEG can generate a high voltage with a low current due to high resistance of piezoelectric materials [1]. In contrast, EMG can generate a large current with a low voltage with smaller dimensions and simpler mechanical structures [17]. Currently, most of the studies focus on the design principle and power generation efficiency of EMG and the research on the low voltage generated by EMG leading to unreliable startup of sensors' circuit system is rarely mentioned in those literatures. Although literature [16] proposed an energy management scheme for PEG, it is difficult to ensure that the energy generated by EMG can provide stable energy guarantee for the sensor's circuitry due to the limited amplitude of the vibration generated by freight trains. Moreover, there is a limited amount of work on the matching between EMG output voltage with sensor energy demand,

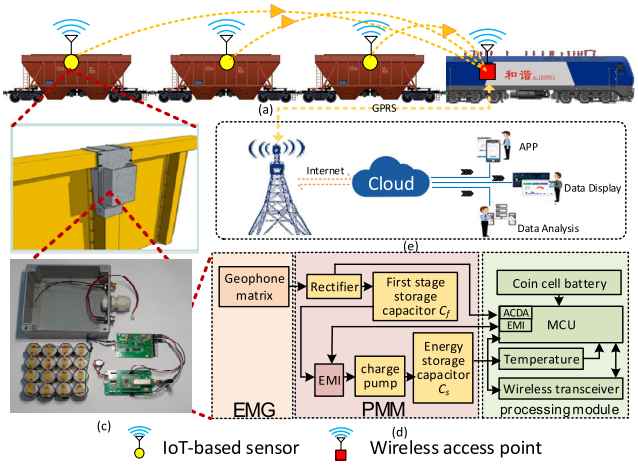

FIGURE 1. (a) Wireless communication network topology. (b) Installation diagram of SpRWMS. (c) The composition of SpRWMS. (d) System architecture of SpRWMS. (e) Application layer network topology architecture.

and the long-term stability of EMG to withstand the demanding conditions of railway environment.

Therefore, the aim of this paper is to propose a SpRWMS solution with high reliability and simple structure to meet the monitoring requirements of railway freight cars in harsh application environments. This paper focuses on the design and implementation of the geophone-based EMG and EMI. In this paper, the purpose of the proposed EMI is to overcome the problem that the electromotive voltage induced by geophone-based EMG is insufficient to drive the sensor circuitry and improve the efficiency of energy conversion.

II. SYSTEM DESCRIPTION AND VIBRATION CHARACTERISTICS ANALYSIS

A. SYSTEM STRUCTURE

The wireless sensor network topology on the freight train and the block diagram of SpRWM are shown in Fig. 1. The wireless access point is installed in the locomotive, used to collect the monitoring results of freight cars which perceived by the SpRWMS mounted on the carriages of freight trains, such as wagon unique code, axle temperature, axle crack detection results, etc., and then transmit this information to a remote server through the public network such as the Internet.

As depicted in Fig 1d the SpRWMS consists of three main components: EMG, PMM and processing module (PM). The EMG constructed by geophones is the power source that can provide the energy supply for the circuitry assembled in SpRWMS, and the PMM is a circuit that converts the energy generated by the EMG into the electrical energy form that can drive the circuit system of the processing module. The processing mode is the core component of SpRWMS, which is responsible for monitoring data collection and processing, wireless data interaction, etc. The design and implementation of these three components will be analyzed in depth below.

Additionally since the geophone can also provide accurate vibration signal source for the ACDA as same as MEMS accelerometer to realize railway axle fatigue crack

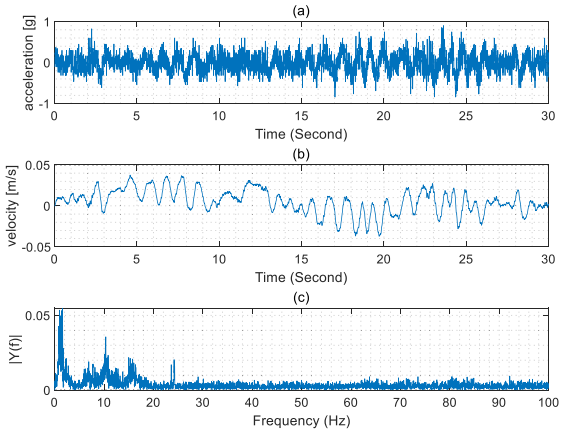

FIGURE 2. Vibration profile measured in a freight train with a velocity of 80 km/h. (a) Example of measured acceleration profile for 30 seconds of travel. (b) The velocity of travel in the vertical direction with respect to the acceleration profile. (c) Fourier transforms performed on the example of vibration profile.

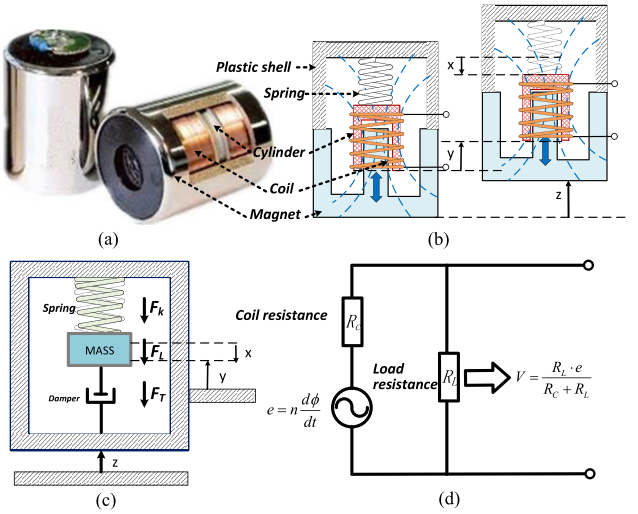

FIGURE 3. (a) Internal structure of the moving-coil geophone. (b) Working principle of the moving-coil geophone. (c) Mechanical model. (d) Equivalent circuit model.

monitoring without any energy consumption [18], this paper also reserves the data acquisition hardware interface for ACDA as shown in Fig 1d Due to space limitations, this paper only focuses on the design and implementation of the geophone-based energy harvesting mechanism, which ensures that the collected energy can guarantee daily energy demand of the circuit system of SpRWMS and improve the energy utilization efficiency as high as possible. Therefore, wagon vibration characteristics and EMG principle are analyzed in detail in order to select the suitable geophone.

B. RAILWAYS VIBRATION CHARACTERISTICS

The EMG in the paper is a device that can convert the mechanical vibration energy of freight cars into the electrical energy from required by the autonomous sensors. In order to analyze the feasibility of our proposed EMG, a data logger consisting of a MCU STM32L053 (ST Semiconductors, Geneva, Switzerland) and a MEMS accelerometer ADXL335 (Analog Devices, Massachusetts, USA) was designed and installed on a carriage of a freight train to record the vibration profiles In the installed data logger, the X-axis of the accelerometer is the direction of travel, the Y-axis is orthogonal to the direction of travel in the horizontal direction, and the Z-axis is the vertical direction.

During the data recording phase, the MCU collects the vibration signals at a sampling rate of 200 Hz and saves them as a contour. Hence, the vibration signals with the frequency of up to 100 Hz can be recorded according to Shannon's law.

Since the geophone is only sensitive in the vertical direction, this paper only focus on the vibration signals along the Z-axis and an example of measured acceleration profiles for a 30 second train of travel is shown in Fig. 2 As shown in Fig. 2 the maximum vibration signal of the measured freight train is in the range of 1g. Therefore, the moving speed in the vertical direction of the freight car is in the range of 0.05m/s based on the measured acceleration profiles according to Newton's law Moreover, the largest vibration responses were found to occur in low frequency band (3–5 Hz), with smaller peaks at 12, 18 and 25 Hz, and the average measured acceleration is about 0.353g and the maximum speed in the vertical direction is about 0.042m/s. Since these data feature of the vibration are very important for the selection of geophones, the following section will deeply analyze the working principle of geophones and provide guidance for the construction of the by combining with above parameters.

C. CONSTRUCTION AND WORKING PRINCIPLE OF GEOPHONE

Generally, the moving-coil geophone is equipped with a spring-mounted mass which moves within a wire coil and a magnet. The electric energy generated by the EMG is converted from the mechanical energy of the relative movement of magnet and coil assembled in the geophone according to Faraday's law of electromagnetic induction, as shown in Fig. 3

The governing dynamic model of the moving-coil geophone can be simplified into a degree-of-freedom model system consisting of mass, spring and damping, as shown in Fig. 3b and Fig. 3c Among them, z is the ground displacement, y is the mass's displacement relative to the ground, x is the relative displacement distance between the magnet and the coil, and the relationship between them is $y = z + x$.

Hence, according to Faraday's law, the relative oscillating motion will cause a change in the magnetic flux inside the coil, and the potential induced in the coil can be expressed as:

$$e = n\frac{d\varphi}{dt} = n\frac{d\varphi}{dx}\cdot\frac{dx}{dt} = s\cdot\frac{dx}{dt}. \quad (1)$$

where e is the induced voltage and $d\phi$ is the magnetic flux$n$ is the number of turns in the coil According to Eq. (1),

the magnitude of the induced voltage is proportional to the displacement velocity of the coil relative to the moving mass. Additionally, the Lorentz force F_L generated by induced current can be express as:

$$F_L = -n\frac{d\phi}{dx}\cdot i = -s\cdot\frac{e}{R_c + R_L} = -\frac{s^2}{R}\cdot\frac{dx}{dt}. \quad (2)$$

where i is the induced current, R_c is coil resistance and R_L is load resistance. According to Newton's second law, there are:

$$\begin{aligned} F_k + F_L + F_T &= -k\cdot x - \frac{s^2}{R}\cdot\frac{dx}{dt} + \mu\frac{dx}{dt} \\ &= M\cdot\frac{d^2y}{dt^2} = M\cdot\left(\frac{d^2z}{dt^2} + \frac{d^2x}{dt^2}\right). \end{aligned} \quad (3)$$

where k is the spring stiffness coefficient and F_k is spring force, M is the mass of body inertia, μ is electromagnetic damping coefficient and F_T is the electromagnetic damping force. According to Eq. (3), it can be derived:

$$\begin{aligned} &\frac{d^2x}{dt^2} + \frac{1}{M}\cdot\left(\mu + \frac{s^2}{R}\right)\cdot\frac{dx}{dt} + \frac{k}{M}x = -\frac{d^2z}{dt^2}. \\ &\Rightarrow \frac{d^2x}{dt^2} + 2h\frac{dx}{dt} + \omega_0^2 x = -\frac{d^2z}{dt^2}. \end{aligned} \quad (4)$$

where $h = (\mu + s^2/R)/2M$ is the damping coefficient, $\omega_0 = \sqrt{K/M}$ is the natural frequency. According to Eq. (1), the voltage across the load resistor is:

$$V = \frac{e}{R_c + R_L}\cdot R_L = \frac{e}{R}\cdot R_L = s\cdot\frac{R_L}{R}\cdot\frac{dx}{dt} = G_0\cdot\frac{dx}{dt}. \quad (5)$$

Hence, substituting the derivative of V with Eq. (3), the rearrangement equation is:

$$\begin{aligned} &\frac{d^2V}{dt^2} + 2h\frac{dV}{dt} + \omega_0^2 V = -G_0\frac{d^3z}{dt^3}. \\ &\Rightarrow \frac{d^2V}{dt^2} + 2D\omega_0\frac{dV}{dt} + \omega_0^2 V = -G_0\frac{d^2Z'}{dt^2}, \\ &(Z' = \frac{dz}{dt}, D = h/\omega_0) \end{aligned} \quad (6)$$

Since the average speed of freight trains is between 80-120Km/h, the electromagnetic damping of geophones installed on the running freight cars is greater than zero according to the analysis results in Chapter 2B Therefore, the transfer function can be obtain by performing the Fourier transform on the Eq. (6) when train is in motion:

$$\begin{aligned} H(\omega) &= |H(j\omega)| = |\frac{V(j\omega)}{Z'(j\omega)}| \\ &= |-\frac{G_0}{\left(1 - \frac{\omega_0^2}{\omega^2}\right) - j2D\frac{\omega_0}{\omega}}| \\ &= \frac{G_0}{\sqrt{\left(1 - \frac{\omega_0^2}{\omega^2}\right)^2 + 4D^2\cdot\frac{\omega_0^2}{\omega^2}}}. \end{aligned} \quad (7)$$

According to Eq. (7), the amplitude-frequency response of geophones can be shown in Fig. 4.

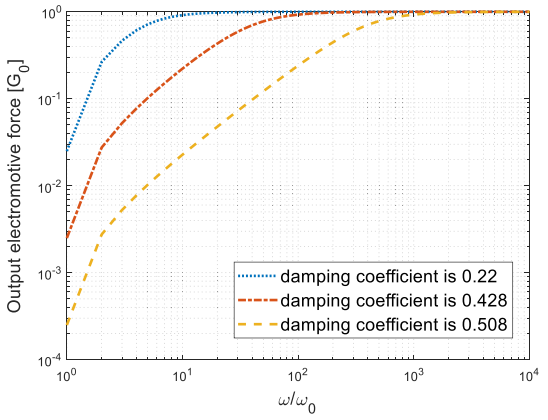

FIGURE 4. Amplitude-frequency response curves of the moving-coil geophone with different damping coefficients.

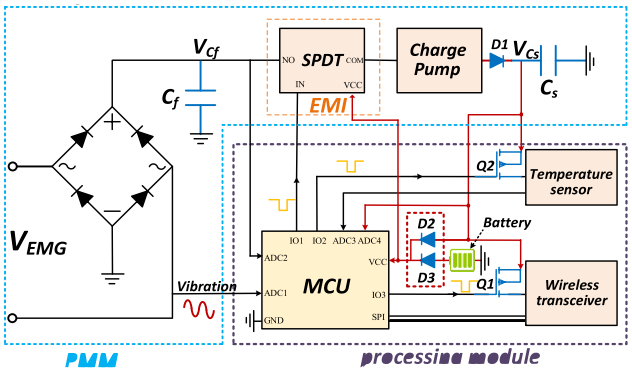

FIGURE 5. Schematic of the customize SpRWMS consisting of the EMI, rectifier and charge pump.

As depicted in Fig. 4 the amplitude-frequency response of geophones is high-pass and the cut-off frequency gradually decreases as the damping coefficient increases. According to the above analysis, since the vibration energy of freight cars is mainly distributed between 3-30 Hz, it is necessary to select a geophone with lower natural frequency and smaller damping coefficient to build the EMG to convert the vibration energy into electrical energy as much as possible. Furthermore, in order to improve the practical value of the EMG proposed in this paper, the geophone should have a high cost performance. Therefore, this paper finally chose the lowest price geophone PS-14X (Sunfull, Weihai, China) [19] that can be purchased on the market to build an EMG, and the price of the geophone is about $ 5. Additionally, the natural frequency sensitivity and damping coefficient of the selected geophone are 14Hz 28V/(m/s) and 0.22, respectively Hence, according to the data feature of train vibration analyzed in section 2B, the maximum output open-circuit voltage e_{max} of the geophone can reach 1.176V.

III. DESIGN AND IMPLEMENTATION

A. CIRCUIT SYSTEM DESIGN

The implementation of the circuit system of SpRWMS is shown in Fig 5. As shown in Fig 5, the circuit system of the SpRWMS consists of the following circuit units:

microcontroller, wireless transceiver temperature sensor full-bridge rectifier, single pole double throw (SPDT) analog switch, charge pump, and storage capacitor.

The microcontroller used in the customized SpRWMS is STM32L053 with a minimum startup voltage of 1.8V, which is used for EMI management, temperature data acquisition, wireless data interaction, and execution of ACDA. The wireless transceiver used is SX1278 (Semtech Corporation, California, USA) with a supply voltage range of 1.8-3.6V, and the temperature sensor is MCP9700 (Microchip Technology, Inc., Arizona, USA) with a minimum startup voltage of 2.3V. Therefore, the customized SpRWMSs can only be started up if the output voltage of the EMI is greater than 2.3V.

From Fig. 5, there are two energy storage capacitors in the SpRWMS, which are the first stage storage capacitor C_f and the energy storage capacitor C_S The function of capacitor C_f is to smooth the voltage output from the rectifier and provide continuous energy for the charge pump. The capacitor C_S is used to provide energy supply to the backend circuit system, such as temperature sensor and wireless transceiver, which are powered by C_s and controlled by MCU via the PMOS transistors. Meanwhile, we introduce a power path management circuit composed of two diodes and CR1220 coin cell battery in SpRWMS to ensure the stability and reliability of the circuit system when the energy stored in C_S cannot power the MCU to perform tasks and execute specific applications. Generally, the MCU is powered by CR1220 when the voltage across C_S is less than that of CR1220, and vice versa. Since the MCU spends most of its life cycle in the sleep mode, the average energy consumption can be as low as 5μA, thus the CR1220 as a supplementary energy source is enough for the energy required for the MCU to complete daily work when there is not enough energy stored in the capacitor C_S.

Moreover, according to the analysis in section 2C the open-circuit voltage output from the geophone is only about 1V which cannot provide enough voltage to drive the circuit system of the autonomous sensor with minimum start-up voltage of 2.3V to operate reliably. Hence, a charge pump TPS60310 (Texas Instruments, Texas, USA) has been introduced into the circuit system of SpRWMS, which has high power conversion efficiency in the voltage range of 0.8V-1.8V. Moreover the TPS60310 can generate an output voltage of 3.3V when the input voltage meets certain conditions.

Nevertheless, since the capacitor has a certain capacitive reactance in regard to the frequency of the signal passing through it, according to Ohm's law, the voltage across the C_f is much smaller than the open circuit voltage generated by the geophone. Therefore, in order to improve the availability of self-powered systems, an EMG constructed by geophone matrix is proposed in this paper.

B. EMG DESIGN

Theoretically the rectified Root Mean Square (RMS) voltage across the capacitor C_f is $e_{max}/\sqrt{2} = 0.83$V. However in reality, during each half cycle the current flows through two diodes so the amplitude of the output voltage is two voltage drops less than the input e_{max} amplitude due to the forward voltage V_F of diodes which may cause the charge pump to fail to start up reliably Moreover, since the geophone's coil resistance is as high as 395Ω, which results in its limited load carrying capacity. Therefore, EMG in the form of a matrix composed of multiple geophones is proposed in this paper, increase the open output circuit voltage of the EMG in series, and reduce the internal resistance of the EMG in parallel to improve the load capacity as shown in Fig. 6.

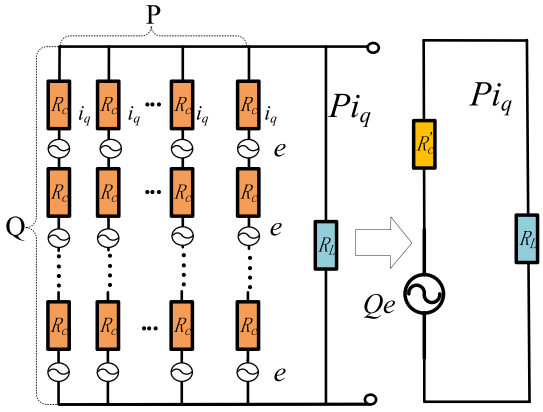

FIGURE 6. The composition principle of EMG and its equivalent circuit system.

After making a compromise between cost and performance, the proposed EMG was eventually built with 16 geophones in this paper. That is, the P value is 4 and the Q value is 4 in Fig. 6. According to Ohm's law, the internal resistance R'_{C} and EMG open circuit voltage V_{EMG} can be obtained:

$$\begin{cases} V_{EMG} = Q \cdot e, \\ R'_{\mathrm{C}} = QR_C//QR_C//QR_C//QR_C. \end{cases} \tag{8}$$

According to Eq. (8) and the previous analysis, the maximum open circuit voltage of V_{EMG} can reach 3.2V, and the resistance of R'_{C} is about 395Ω.

C. EMI DESIGN

According to the data sheet of the charge pump TPS6031, the conversion efficiency increases as the input voltage increases. In other words, the lower the input voltage, the greater the energy loss. Since the voltage output from the EMG is related to the amplitude and frequency of the vibration of freight trains, the output voltage of the EMG is very low when the freight trains are slow, and may even be close to the start-up threshold voltage of the charge pump. Nevertheless, the worst thing is that although the TPS60310 cannot be started when input voltage is below its start-up threshold voltage, the built-in and connected sub-circuits still draw energy from the first stage storage capacitor C_f, which ultimately fails to start the charge pump, and then in turn causes unnecessary energy loss.

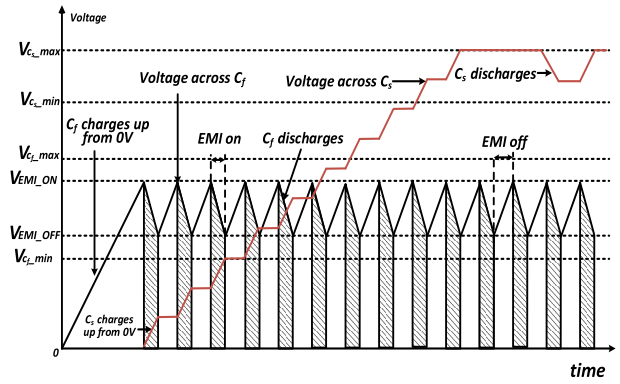

FIGURE 7. An illustration of the voltages across C_f and C_s.

Therefore, this paper includes an EMI circuit composed of low-power SPDT analog switch RS2257 (RUNIC Technology, Wuxi, China) with 0.6Ω on-state resistance to solve the problem of energy loss caused by the above-mentioned situation as shown in Fig. 5. In our proposed SpRWMS prototype, the normally-open (NO) terminal and common (COM) terminal of the SPDT are connected to the capacitor C_f and the charge pump, respectively. A GPIO of the microcontroller is connected to the digital control (IN) pin of the SPDT, and the connectivity between the capacitor C_f and the charge pump is controlled by the microcontroller.

The design principle of the proposed EMI circuit is that when the voltage across the first stage storage capacitor C_f is greater than a specific voltage threshold V_{EMI_ON}, the voltage level of IN terminal of the SPDT will be set to a logic-1 state by MCU, which causes the impedance between the NO terminal and COM terminal of SPDT to tend to 0.6Ω hence, the charge pump is activated to boost the voltage across C_f up to 3.3V and charge the energy storage capacitor C_s Similarly, when the voltage across capacitor C_f is less than V_{EMI_OFF}, the connectivity between NO terminal and COM terminal of SPDT will be turned off by MCU, that is, the impedance between capacitor C_f and charge pump is infinite, and the charge pump will stop working. The relationship between the voltage across C_f and C_s is shown in Fig. 7.

D. THRESHOLD AND STORAGE CAPACITOR SELECTION

According to the data sheet of charge pump, the maximum voltage $V_{\mathrm{cs\_max}}$ across C_s capacitor is approximately equal to 3.3V when the input voltage meets certain requirement. The minimum voltage $V_{\mathrm{cs\_min}}$ is the lowest voltage threshold that can start the circuitry and the value is 2.3V in this paper, in order to provide an extra margin to the energy availability for the MCU to perform any task successfully before V_{CS} drops below $V_{\mathrm{cs\_min}}$, the capacitance of the capacitor C_S must satisfy:

$$\frac{1}{2}C_s V_{c_s\_max}^2 - \frac{1}{2}C_s V_{c_s\_min}^2 \geq E_{required}. \tag{9}$$

where $E_{required}$ is the overall energy required for the SpRWMS in a day, and it can be expressed as:

$$E_{required} = E_{sleep} + E_{ADC} + E_{Sensor} + E_{RF\_TX}. \tag{10}$$

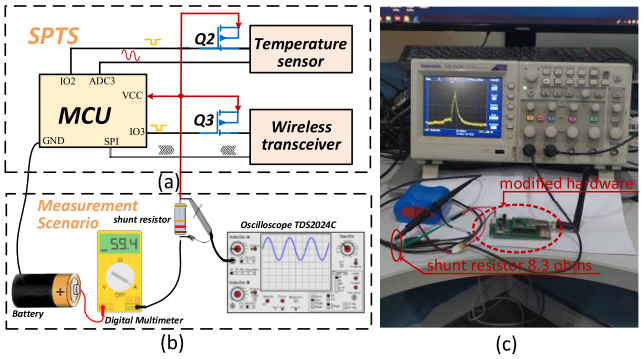

FIGURE 8. (a) Schematic of modified hardware system. (b) Schematic diagram of the measurement scenario consisting of a multimeter and an oscilloscope. (c) Actual measurement scenario.

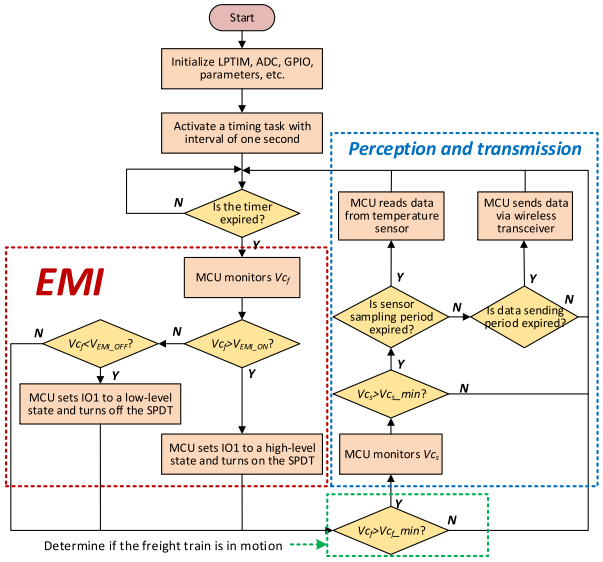

FIGURE 9. The embedded program implementation flow chart of the proposed SpRWMS prototype.

where E_{sleep} and E_{ADC} are the energy consumption when the MCU is in sleep mode and its built-in ADC is in the sampling mode, respectively. E_{Sensor} is the quiescent energy consumption of the temperature sensor, and E_{RF_TX} is the energy consumption of the wireless transceiver to transmit 32 data when the transmit power is 10dBm and data rate is 300kbps. According to Joule's law, the above four energy consumption can be evaluated:

$$E(t_n) = \sum_{k=1}^{n} V(t_k) I(t_k) \Delta t. \tag{11}$$

where $V(t_k)I(t_k)$ and Δt are the voltage, current and activation duration of each task execution.

In order to get the total required energy $E_{required}$ of the SpRWMS in a day, we need to build an actual measurement scenario to measure the individual energy consumption of each circuit unit as shown in Fig. 8b Firstly, the EMI, full-bridge rectifier, storage capacitors, and coin battery were removed from SpRWMS circuit as shown in Fig. 8a. Then,

a UNI-T UT61E digital Multi-Meter was used to measure the quiescent current of temperature sensor and the sleep current of the microcontroller which change more slowly An oscilloscope was used to measure the activation duration and the voltage dropped across a shunt resistance due to the operating current of wireless transceiver with the transient characteristic Finally, the current consumed by each circuit unit can be inferred based on Ohm's Law (I = V/R) and the above measurement parameters.

Using above method, E_{ADC}, E_{Sensor} and E_{RF_TX} have been found to be 13.2μJ, 21.3μJ and 1.386mJ respectively in the studied case. Since the sleep current is as low as 1μA, for the convenience of calculation, E_{sleep} is abandoned in this paper.

Additionally, in the customized SpRWMS, the ADC integrated in the MCU monitors $V_{CS}V_{Cf}$, and the output voltage of the temperature sensor at a frequency of 5 seconds and the wireless transceiver sends data at 24-hour intervals or when an temperature over-threshold alarm signal is detected that is, the energy in the storage capacitor C_S must support the energy required for two consecutive wireless packet transmissions and temperature sensor data acquisition. Hence, according to Eq. (9) and Eq. (10), the capacitance of C_s is at least greater than 590μF Finally two 470μF tantalum capacitors were selected as storage capacitors to customize SpRWMS to ensure its stability.

Additionally, since V_{Cf} determines the energy conversion efficiency of the charge pump, the performance of PMM will affected by the choice of the capacitor C_f In this paper, a tantalum capacitor is also used as the first-stage energy storage capacitor due to its equivalent series resistance (ESR) is as low as 0.06Ω. Hence, the maximum voltage $V_{c_f\_max}$ is related to the amplitude-frequency response of V_{EMG} and the capacitance of C_f, there is:

$$V_{c_f\_max} = |V_{EMG}| \cdot \frac{R_L}{R + R_L} = |V_{EMG}| \cdot \frac{1/2\pi fC}{R + 1/2\pi fC}. \quad (12)$$

where f and C are the main frequency components of V_{EMG} and the capacitance of C_f, respectively. In this paper, the voltage threshold $V_{c_f\_max}$ is set to 1.1V, hence, according to previous analysis, the capacitance selection range of the capacitor C_f is between 1μF and 33μF, and a tantalum capacitor with 33μF is finally selected as the first-stage energy storage capacitor.

E. ALGORITHM IMPLEMENTATION

This section will focus on the implementation of the strategy algorithms embedded in the MCU, and the implementation flow chart is shown in Fig. 9 In the proposed algorithm, the ADC in the MCU reads voltage V_{Cf} in the interrupt callback function which triggered by the Low Power Timer (LPTIM) assembled in MCU periodically, and uses the EMI program to judge whether there is enough energy in the capacitor C_f for the charge pump to carry out energy conversion, that is, V_{Cf} is larger than V_{EMI_ON}. Generally, if V_{Cf} is greater than V_{EMI_ON}, the SPDT analog switch will be turned on by EMI program, and when V_{Cf} is less than V_{EMI_OFF}, the MCU will turn off SPDT analog switch Hence, only when V_{Cf} satisfies $V_{EMI\_OFF} < V_{Cf} < V_{EMI\_ON}$, the energy in capacitor C_f can be transferred to the capacitor C_S.

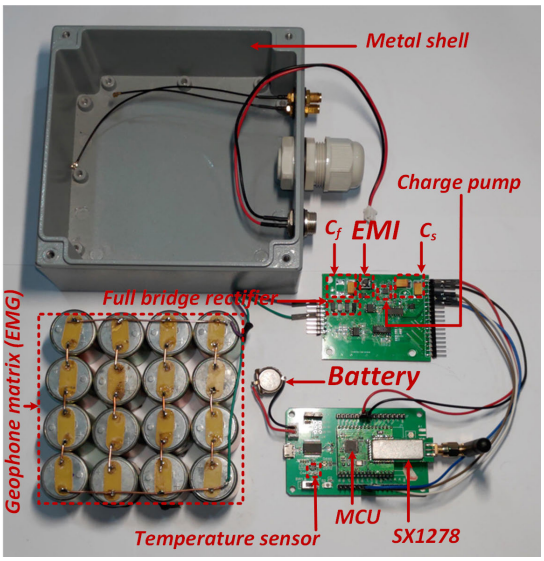

FIGURE 10. The proposed SpRWMS prototype consisting of the geophone matrix (EMG), PMM, processing module, and metal shell.

Additionally, the MCU also monitors V_{CS} to judge whether the energy in the capacitor C_S provides enough energy for the wireless transceiver and temperature sensor to perform their respective tasks successfully Moreover, since the data features of sensor output reflected by the monitoring object such as axle fatigue crack and axle temperature are effective only when the train is in motion, hence, this paper determines whether to perform the perception and transmission task by monitoring the signal characteristics of V_{Cf} as shown in Fig. 5.

IV. EXPERIMENTAL RESULTS AND DISCUSSIONS

A. SPRWMS PROTOTYPE

In order to understand the benefits of our proposed SpRWMS solution for application scenarios such as freight train carriage monitoring scenarios, a SpRWMS prototype with EMG and EMI was customized experimentally as shown in Fig.10.

As can be seen from Fig. 10, the SpRWMS prototype, consisting of the energy harvester, storage capacitor, SPDT charge pump, wireless transceiver, micro-controller and temperature sensor, was integrated into a rugged enclosure and mounted to the suspension on the wagon of a freight train as shown in Fig. 1.

B. EXPERIMENTAL SETUP

In order to understand the advantages of the EMI approaches for the SpRWMS prototype, characterizations and comparisons of 2 different scenarios have been performed in the evaluation phase. In scenario 1, the EMI block of the customized SpRWMS prototype is removed, which means that the SPDT analog switch is permanently turned on.

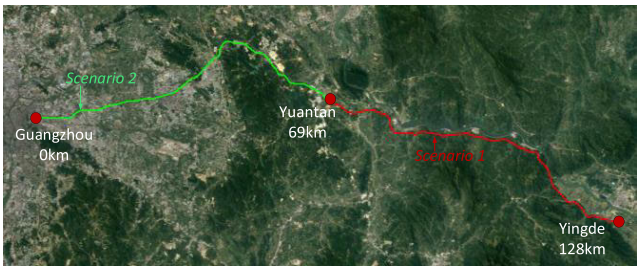

FIGURE 11. Actual test run route for prototype field trail.

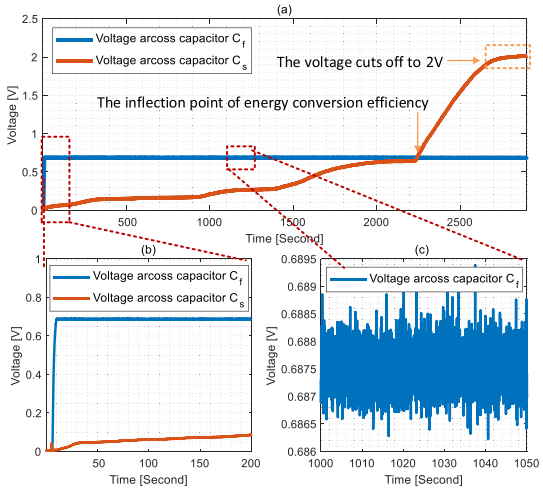

FIGURE 12. (a) The relationship between V_{Cf} and V_{CS} without EMI. (b) Enlarged view of the changes of V_{Cf} and V_{CS} during startup. (c) Enlarged view of the voltages across capacitor C_f.

In scenario 2, the MCU periodically monitors the voltage across C_f at intervals of one second and controls the logic level on the IN terminal of the SPDT according to flowchart as shown in Fig. 9.

In order to compare the performance of the energy harvesting approach proposed in this paper under the above two conditions the relevant experimental results were obtained by means of a freight train test run on the rails from GuangZhou (0 km) to Yingde (128 km) with stopping at Yuantan (69 km) in China as shown in Fig. 11.

Meanwhile, a NI9234 data acquisition module (National Instruments, Texas, USA) is used to read the voltages across the capacitors C_f and C_S in the experiment, and the monitoring results are recorded in the computer hard disk drive. Moreover, to make fair comparisons between scenarios 1 and 2, the active and sleeping duration of scenario 2 is configured to be the same as scenario 1 and the temperature sensor and wireless transceiver are also placed in permanent sleep state in both verification scenarios.

C. EMI PERFORMANCE EVALUATION

As can be seen from Fig. 12, in the evaluation scenario 1 without EMI, the charge pump can transfer and boost the energy stored in the first stage storage capacitor C_f to C_S

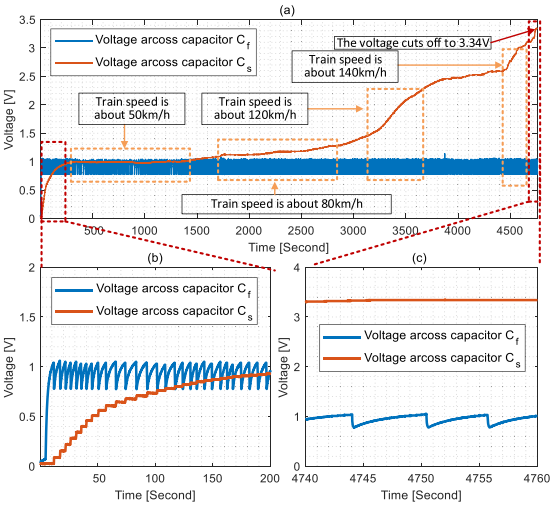

FIGURE 13. (a) The relationship between V_{Cf} and V_{CS} of the proposed SpRWMS prototype with EMI. (b) Enlarged view of the changes of V_{Cf} and V_{CS} during startup. (c) The cut-off voltage value of V_{Cf} and V_{CS}.

at any time, and the reliable start-up voltage charge pump is around 0.7V. Additionally, according to the data sheet of the charge pump chip, the input voltage near the start-up voltage threshold will cause the built-in switching circuit to continuously ping-pong switch, which leads to a large energy loss.

Moreover, the energy conversion efficiency tends to increase with the increase of the input voltage according to the data sheet, that is, the higher the input voltage, the smaller the energy loss in the process of transferring energy from C_f to C_S. Therefore, the loss of energy due to conversion efficiency and frequent switching operations causes the charge pump output to fail to reach the nominally achievable voltage. From Fig. 12, the experiment results have shown that the voltage V_{CS} cannot continue to rise when it is up to 2V. According to previous analysis, it can be found that this voltage cannot drive all the electronic components in the SpRWMS and can maintain their operation reliably.

The experimental results of evaluation scenario 2 with EMI are shown in Fig. 13 From Fig. 13, as the speed of the freight train increases, so does the amplitude of the vibration, which in turn causes the EMG to generate much more electric energy. As can be seen from Fig. 13, the SpRWMS prototype has better performance when the vehicle speed is greater than 50km/h Generally, the average speed of freight trains is mostly between 80-140km/h in China, so the proposed SpRWMS solution has a strong practical significance.

As shown in Fig. 12 and Fig. 13, the obvious difference between verification scenarios 1 and 2 is the cutoff voltage across capacitor C_S and energy transfer mode. The cutoff voltage V_{CS} in the scenario 2 can reach the nominal output voltage of charge pump with the value of 3.3V, while that of evaluation scenario is only 2V. Therefore, the EMI mechanism proposed in this paper can meet the energy form required by SpRWMS circuits and provide reliable energy supply guarantee for SPRWMS.

Additionally, from the comparison of Fig. 12 and Fig. 13, the SpRWMS prototype without EMI takes less time to charge the capacitor C_S to 2V than that of the prototype with EMI. The main reason may be that after the introduction of EMI, frequent switching of the analog switch leads to energy loss. But in general, the energy generated by EMG can be effectively converted into the energy specifications required by SpRWMS circuitry through the EMI introduced in this paper. Therefore, the method proposed in this paper can provide guiding significance for the realization of the monitoring sensor for freight trains.

V. CONCLUSION

Since the wagons of freight trains have no power supply and the operating environment is very harsh for electronic equipment, this paper proposes a self-powered railway wagon monitoring sensor solution with high reliability and simple structure, which uses the geophone to design and implement the EMG, and develop corresponding energy management circuit and embedded strategy algorithms to convert as much as possible of the electric energy generated by the geophones into storage capacitors that can support the reliable operation of IoT-based autonomous monitoring sensors Finally, field experiments on a trail run freight train prove that the solution proposed in this paper has high use value.

However, the proposed energy harvesting approach still has some shortcomings and needs to be improved in the future Firstly, the proposed approach has only been tested in middle of the upper side beam of the wagon, which may not be the optimal place, thus, future work will evaluate the efficiency of the proposed approach in other places in order to obtain the most reasonable installation location. Secondly, this paper does not make a reasonable explanation for the selection of the voltage thresholds V_{EMI_ON} and V_{EMI_OFF}, so the selection of these parameters will be studied and optimized in the future. Similarly, system integration and reliability issues cannot be ignored because the sensors on the freight cars must be subjected to very harsh environmental conditions over long periods.

REFERENCES

[1] S. Bradai, S. Naifar, C. Viehweger, and O. Kanoun, "Electromagnetic vibration energy harvesting for railway applications," in *Proc. MATEC Web Conf.*, vol. 148, 2018, p. 12004.
[2] E. Bernal, M. Spiryagin, and C. Cole, "Onboard condition monitoring sensors, systems and techniques for freight railway vehicles: A review," *IEEE Sensors J.*, vol. 19, no. 1, pp. 4–24, Jan. 2019.
[3] O. Brignole, C. Cavalletti, G. Lauro, A. Maresca, N. Mazzino, M. Balato, A. Buonomo, L. Costanzo, M. Giorgio, R. Langella, A. L. Schiavo, D. Scaldarella, A. Smoraldi, A. Testa, L. Verde, and M. Vitelli, "Experimental analysis of mechanical vibrations and wind speed for a rail vehicle WSN fed by energy harvesters," in *Proc. AEIT Int. Annu. Conf. (AEIT)*, Naples, Italy, Oct. 2015, pp. 1–6.
[4] V. G. Cleante, M. J. Brennan, G. Gatti, and D. J. Thompson, "On the target frequency for harvesting energy from track vibrations due to passing trains," *Mech. Syst. Signal Process.*, vol. 114, pp. 212–223, Jan. 2019.
[5] M. Macucci, S. Di Pascoli, P. Marconcini, and B. Tellini, "Derailment detection and data collection in freight trains, based on a wireless sensor network," *IEEE Trans. Instrum. Meas.*, vol. 65, no. 9, pp. 1977–1987, Sep. 2016.
[6] C. Wei and X. Jing, "A comprehensive review on vibration energy harvesting: Modelling and realization," *Renew. Sustain. Energy Rev.*, vol. 74, pp. 1–18, Jul. 2017.
[7] D. Song, H. Jang, S. B. Kim, and T. H. Sung, "Piezoelectric energy harvesting system for the vertical vibration of superconducting Maglev train," *J. Electroceram.*, vol. 31, nos. 1–2, pp. 35–41, Oct. 2013.
[8] A. Mouapi, N. Hakem, N. Kandil, and G. V. Kamani, "Energy harvesting design for autonomous wireless sensors network applied to trains," in *Proc. IEEE Int. Ultrason. Symp. (IUS)*, Sep. 2016, pp. 1–4.
[9] M. Gao, P. Wang, Y. Cao, R. Chen, and D. Cai, "Design and verification of a rail-borne energy harvester for powering wireless sensor networks in the railway industry," *IEEE Trans. Intell. Transp. Syst.*, vol. 18, no. 6, pp. 1596–1609, Jun. 2017.
[10] Z. Hadas and C. Ondrusek, "Nonlinear spring-less electromagnetic vibration energy harvesting system," *Eur. Phys. J. Special Topics*, vol. 224, nos. 14–15, pp. 2881–2896, Nov. 2015.
[11] J. Y. Cho, S. Jeong, H. Jabbar, Y. Song, J. H. Ahn, J. H. Kim, H. J. Jung, H. H. Yoo, and T. H. Sung, "Piezoelectric energy harvesting system with magnetic pendulum movement for self-powered safety sensor of trains," *Sens. Actuators A, Phys.*, vol. 250, pp. 210–218, Oct. 2016.
[12] D. Song, C. H. Yang, S. K. Hong, S. B. Kim, M. S. Woo, and T. H. Sung, "Feasibility study on application of piezoelectricity to convert vibrations of Korea train express," in *Proc. ISAF-ECAPD-PFM*, Aveiro, Portugal, 2012, pp. 1–4.
[13] M. Koch, M. Kurch, and D. Mayer, "Methodical design approach and field test of a self-powered train hot box detector," *Int. J. Railway Technol.*, vol. 1, no. 4, pp. 19–38, 2012.
[14] D. Upadrashta and Y. Yang, "Experimental investigation of performance reliability of macro fiber composite for piezoelectric energy harvesting applications," *Sens. Actuators A, Phys.*, vol. 244, pp. 223–232, Jun. 2016.
[15] M. Gao, P. Wang, Y. Wang, and L. Yao, "Self-powered ZigBee wireless sensor nodes for railway condition monitoring," *IEEE Trans. Intell. Transp. Syst.*, vol. 19, no. 3, pp. 900–909, Mar. 2018.
[16] T. Ruan, Z. J. Chew, and M. Zhu, "Energy-aware approaches for energy harvesting powered wireless sensor nodes," *IEEE Sensors J.*, vol. 17, no. 7, pp. 2165–2173, Apr. 2017.
[17] L. Jin, W. Deng, Y. Su, Z. Xu, H. Meng, B. Wang, H. Zhang, B. Zhang, L. Zhang, X. Xiao, M. Zhu, and W. Yang, "Self-powered wireless smart sensor based on maglev porous nanogenerator for train monitoring system," *Nano Energy*, vol. 38, pp. 185–192, Aug. 2017.
[18] M. Gómez, E. Corral, C. Castejón, and J. García-Prada, "Effective crack detection in railway axles using vibration signals and WPT energy," *Sensors*, vol. 18, no. 5, p. 1603, May 2018.
[19] *PS-14X, Data Sheet*. Accessed: Nov. 2019. [Online]. Available: https://www.sunfull.com/cp/html/?60.html

WEI HE received the Ph.D. degree in communication and information system from the University of Chinese Academy of Sciences, in 2013. He is currently an Associate Professor with the Shanghai Institute of Microsystem and Information Technology, Chinese Academy of Sciences, Shanghai, China. His research interests include wireless communication systems, sensor networks, and information fusion.

WEIZHONG SHI received the Ph.D. degree in mechanical and electronic engineering from the Beijing University of Technology, in 2004. He is currently the Chairman and a Senior Engineer of China Railway Information Technology Company, Ltd. His research interest includes information and communication signal technology.

JIANWEI LE received the master's degree in computer science and engineering from the Hong Kong University of Science and Technology, in 2008. He is currently an Associate Senior Engineer of China Railway Information Technology Company, Ltd. His research interests include the Internet of Things and AI technology.

HUI LI received the bachelor's degree in railway construction and operation management from Central South University, in 2001. He is currently the General Manager of Fujian Fuzhou Railway Local Railway Development Company, Ltd.

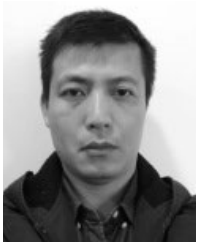

RUNZE MA received the Ph.D. degree in communication and information system from the University of Chinese Academy of Sciences, in 2012. He is currently an Intermediate Engineer of the Shanghai Institute of Microsystem and Information Technology, Chinese Academy of Sciences. His research interests include MEMS-based integrated navigation and array signal processing technology.